Biochimica et Biophysica Acta, 1151 (1993) 127–136

BBAMEM 76068

Interaction of myelin basic protein with single bilayers on a solid support: an NMR, DSC and polarized infrared ATR study

Herbert M. Reinl and Thomas M. Bayerl

Technische Universität München, Physik Department E22, Garching (Germany)

(Received 10 February 1993)
(Revised manuscript received 2 June 1993)

Key words: Protein–lipid interaction; Supported bilayer; FTIR; NMR; DSC; Order parameter

The interaction of myelin basic protein (MBP) with single bilayers on a solid support (planar and spherical support) is studied by deuterium nuclear magnetic resonance (^{2}H-NMR), differential scanning calorimetry (DSC) and polarized attenuated total reflection infrared spectroscopy (ATR-IR). The single bilayer consisted of either DMPC or of a binary mixture of DMPC with 10–20 mol% of an acidic phospholipid (DMPG, DMPS or DMPA). All methods applied indicate that MBP strongly interacts with the binary lipid systems but not with the pure DMPC bilayers. The interaction is predominantly electrostatic in nature and does not depend on the choice of a particular acidic lipid (for the binary systems). In particular, the results give no indication for a hydrophobic interaction of MBP with the membrane. Our data provide evidence that, in contrast to previous findings, no demixing and/or domain formation in the binary systems is induced due to the MBP coupling. The infrared order parameter was determined for both lipid components of the binary systems and shows a remarkable change for both lipids due to the interaction with MBP while the NMR order parameter remained essentially unchanged. This is discussed in terms of the different timescales characteristic for both methods. The single supported bilayer responds to the MBP coupling as a whole although only 50% of the bilayer surface is accessible to the protein, indicating a strong coupling between the two bilayer leaflets via the hydrophobic chain region. Moreover, the asymmetric coupling of MBP to the single supported bilayer does not result in a significant redistribution of lipids between the two bilayer leaflets. NMR relaxation time measurements in the headgroup and chain region of DMPG and DMPC suggest that the lateral diffusion coefficient of the acidic lipid decreases significantly due to the coupling with MBP while the zwitterionic DMPC is not affected.

Introduction

The myelin membrane surrounds the axons of the nervous system and its integrity plays a vital role for proper signal transmission. The importance of the myelin proteins and their interaction with the membrane for the stabilization of the myelin sheet structure is not yet fully understood.

Myelin basic protein (MBP), one of the main protein constituents of the myelin membrane (it accounts for approx. 30 wt% of the total myelin protein), has been established to interact with lipid membranes containing acidic phospholipids mainly by electrostatic interaction using a variety of physical and biochemical methods (for a review, cf., Refs. 1, 2 and 3). Whether MBP exhibits additionally a hydrophobic interaction with bilayers (as suggested in Refs. 1, 4 and 5) due to the presence of a number of hydrophobic residues that are distributed throughout the MBP sequence and its potential to cause the formation of domain structures in binary lipid mixtures is still controversial [3,6,7]. Another important question arises from the fact that MBP couples to the myelin membrane from the cytoplasmic side only. The effect of this asymmetric binding on the structure of the membrane (e.g., an asymmetric lipid distribution between the two bilayer leaflets due to the MBP coupling) has not been addressed yet. Finally, the effect of the MBP interaction on the dynamics of the lipid constituents of the membrane is largely unknown.

A further complication for the comparison of the data published so far on the MBP–lipid bilayer interaction is that all of these studies were done with model systems such as multilamellar and unilamellar vesicles which could be themselves prone to morphological changes due to the interaction with MBP (e.g., size changes or changes of their multilamellarity). Moreover, such model systems do not permit study of the effect of asymmetric MBP binding to bilayers, since both bilayer leaflets are in general equally accessible to the protein.

Correspondence to: T.M. Bayerl, Technische Universität München, Physik Department E22, James-Franck-Strasse, D-W 8046 Garching, Germany.

Single lipid bilayers on a solid support are a model system that can overcome most of the shortcomings of vesicles for studies of protein–lipid interaction. To date, their use (in the form of planar supported membranes) has been restricted mainly to fluorescence applications [8]. The recent introduction of single bilayers on a spherical support enables the use of this well defined membrane model system for spectroscopic studies employing FTIR and DSC [9] as well as broadline NMR techniques [10,11]. There are some unique features of single bilayers on a solid support for studies of protein–lipid interaction.

(i) The interaction of the water soluble protein with the bilayer takes place asymmetrically, i.e., only the leaflet directed to the bulk water phase is accessible to the protein. A similar situation can be found in myelin membranes where the MBP coupling to the membrane is strictly asymmetric.

(ii) Owing to their geometrically well defined nature, the supported systems are superior to multilamellar vesicles since the former offer 50% of their bilayer surface for protein coupling whereas for MLVs the surface accessiblity for proteins is ill-defined. Moreover, the solid support inhibits possible changes of the membrane morphology due to interactions with the protein.

(iii) Finally, since supported bilayers can be easily washed (spherical supported vesicles (SSVs)) or flushed (single bilayers on a planar support) with buffer, the coupling properties of the proteins to the bilayer can be studied in detail regarding variations of the ionic strength and the pH value of the surrounding buffer solution on the same sample.

Using both planar and spherical supported single bilayers we studied the interaction of MBP with membranes employing powerful spectroscopic techniques. The solid support ensures that the membrane geometry cannot change due to the presence of negatively charged lipids in the bilayer or to the coupling of MBP to the bilayer. We present for the first time DSC, NMR and FTIR data obtained for binary lipid mixtures in single bilayers with and without coupled protein. The combination of the methods applied and the advantageous features of the model system allow us to address a number of open questions concerning MBP–lipid bilayer interactions as discussed above.

Materials and Methods

Materials

The phospholipids DMPC, DMPG, DMPS, DMPA, DMPG-d_{54} were purchased from Avanti Polar Lipids and used without further purification. Selectively headgroup-deuterated 1,2-Dimyristoyl-*sn*-glycero-3-phospho[α-$^2H_2$]glycerol (DMPG-d_2) was prepared according to a procedure described in Ref. 12. Myelin basic protein was prepared from bovine brain white matter by the method of Cheifetz and Moscarello [2]. Silica beads for the preparation of spherical supported vesicles were obtained as a gift from Dr. Müller from the Degussa Research laboratories (Degussa AG, Hanau, Germany).

Preparation of model membranes

All lipid preparations were done in a 50 mM Hepes buffer at pH 7.0, adjusted with NaOH, containing 50 mM NaCl.

For multilamellar vesicle (MLV) preparation the corresponding proportions of dry lipid were weighed in glass test tubes, dissolved in chloroform (5 mg/ml), dried under a stream of nitrogen, followed by overnight vacuum desiccation. The lipid film was then redispersed in 50 mM Hepes buffer (pH 7) at a concentration of 20 mg/ml and incubated at 40°C for 30 min under gentle vortexing. For ^{2}H-NMR experiments deuterium-depleted water was used.

Small unilamellar vesicles (SUV) were obtained by sonicating the MLV suspension with a titanium rod sonifier until an optically transparent vesicle solution with an average vesicle diameter of less than 100 nm (measured by dynamic light scattering) was obtained. The SUV solution was then centrifuged in a table top centrifuge in order to remove titanium dust contamination from the sonifier rod.

Spherical supported vesicles (SSV) were prepared by condensation of small unilamellar vesicles on silica beads of 640 ± 40 nm diameter according to procedures described in detail previously [10,13,14].

Single planar bilayer (SPB) were obtained by condensation of SUV on both large faces of a silicon ATR plate inside a homebuilt FTIR sample cell (depicted in Fig. 4). Approx. 10 ml SUV solution (lipid concentration 1 mg/ml) was filled into the cell by means of a syringe. A circulating external water bath kept the temperature of the cell above the phase transition temperature of the injected SUV solution during the SPB preparation. After a 2 min equilibration of the SUV solution inside the cell, the latter was thoroughly flushed with approx. 100 ml buffer using a peristaltic pump in order to remove all SUVs in the bulk solution. For measurements in the presence of MBP, the cell was then flushed with 10 ml protein solution (MBP concentration 0.1 mg/ml) and, after 2 min equilibration, again flushed with 100 ml buffer. This procedure ensured that only MBP coupled to the SPB remained in the cell. The intensity of the lipid signals did not change due to the presence of MBP or to the flushing.

FTIR

Infrared spectra were obtained with a Nicolet 60 SXR Fourier transform infrared spectrometer equipped with a MCT detector and a vertical attenuated total

reflection (ATR) unit. Polarization of the infrared light was achieved by a KRS5 grid wire polarizer (LOT, Darmstadt, Germany). Unless indicated otherwise, 500 scans were acquired at a resolution of 2 cm^{-1} and apodized by a Happ-Genzel function prior to Fourier transform. The background and reference (water) spectra were recorded separately at the corresponding temperatures and the latter was interactively subtracted from the sample spectra. The frequency of the methylene stretching vibration was determined as the maximum of the corresponding band. A vertically arranged $52 \times 20 \times 2$ mm, 45° aperture angle silicon crystal was used as the ATR element inside the homebuilt sample cell (depicted in Fig. 4). The temperature of the sample was measured with a Pt 100 thermocouple inside the ATR assembly and was controlled by an external water bath with an accuracy of ± 0.1 C°. Both temperature and polarization settings were controlled by a computer subsystem connected to the acquisition computer.

The order parameter $\langle S_{IR} \rangle$ and the average orientation angle β were calculated from the dichroic ratio D of the symmetric methylene stretching vibration band of the SPB. $D = A_{\parallel}/A_{\perp}$ is defined as the ratio of the absorption polarized parallel to the plane of incidence to that perpendicular to this plane [15]. The electric field amplitudes E_x, E_y and E_z of the evanescent field on the ATR crystal were calculated in the limit of the thin-film approximation [16] using the following refractive indices: $n_1 = 3.42$ (silicon ATR plate), $n_2 = 1.5$ (fatty acyl region of the single bilayer) and $n_3 = 1.33$ (bulk phase). Here the amplitudes E_x and E_y are the in-plane components and E_z is the out-of-plane (normal to the ATR plate) electric field component of the evanescent field. Since the transition dipolar moment of the methylene stretching vibration of an all-*trans* fatty acyl chain is oriented perpendicular to the chain long axis (the latter corresponds to the molecular director axis of the lipid assuming an axially symmetric molecule), the averaged order parameter $\langle S_{IR} \rangle$ is determined by the fluctuations of the director axis about the normal (E_z direction) of the ATR plate [17,18]:

$$\langle S_{IR} \rangle = \frac{2(E_x^2 - DE_y^2 + E_z^2)}{E_x^2 - DE_y^2 - 2E_z^2} \tag{1}$$

The angular dependence of the order parameter on the angle β between the z-axis and the direction of the molecular director is then given by the well known formula

$$\langle S_{IR} \rangle = \tfrac{1}{2}(3\langle \cos^2\beta \rangle - 1) \tag{2}$$

which enables the calculation of the average orientation angle of the single bilayer with respect to the ATR plate normal (z-axis) in the limit of axially symmetric molecules.

DSC

High-sensitivity DSC measurements were performed with two devices: A MC-2 microcalorimeter (Microcal, Amherst, MA) at a scan rate of 30 C°/h (ascending temperature mode only) and a Hart Scientific microcalorimeter (Hart Scientific, Utah, USA) at a scan rate of 15 C°/h. The latter device was used in both the ascending and descending temperature modes. No significant differences in the DSC endotherms were observed for the two scanning modes (with exception of the pronounced hysteresis for SSV systems as compared to MLV reported previously [9]) regarding the effect of the MBP coupling to the bilayer. The lipid concentration of the DSC samples was 1.5 mg/ml.

NMR

Deuterium NMR experiments were performed at 61 MHz using a Varian VXR-400S spectrometer equipped with a high-power probe. All spectra were obtained using the quadrupolar echo technique with a pulse separation of 20 μs and two 90° pulses of 6 μs duration. The repetition time for successive pulse sequences was 200 ms and 8K data points were collected with a dwell time of 1 μs. For spherical supported vesicles 5000 scans were acquired (1000 scans for multilamellar vesicles). All experiments were done on resonance with a 8 cyclops pulse cycling sequence and no phase corrections were performed. An exponential corresponding to a 50 Hz line broadening was applied to the FID signal prior to taking Fourier transforms. The temperature of the sample was controlled by a Varian temperature control unit and was constant within ± 0.5 C°.

The average ^{2}H-NMR order parameter $\langle S_{NMR} \rangle$ for a perdeuterated acyl chain containing N carbon atoms is given by the arithmetic average of the individual methylene order parameters $|S_{CD}|$ along the chain

$$\langle S_{NMR} \rangle = \frac{1}{N-1} \sum_{n=2}^{N} |S_{CD}(n)| \tag{3}$$

and can be obtained from the average quadrupolar splitting $\langle \Delta\nu_Q \rangle$ (corresponding to the first moment of the ^{2}H-NMR lineshape) according to

$$\langle \Delta\nu_Q \rangle = -\frac{3}{2} \frac{e^2qQ}{2\pi h} P_2(\cos\beta) \langle S_{NMR} \rangle \tag{4}$$

Transverse relaxation time T_2^{qe} measurements were performed by increasing the separation time τ between the $\pi/2$ pulses in 8 steps up to 300 μs. Semilogarithmic plots of the normalized intensity at the top of the echo versus the time $t = 2\tau$ yielded linear depen-

dences for both multilamellar vesicles and SSVs which gave T_2^{qe}.

Results

DSC measurements

Fig. 1A shows DSC endotherms of DMPC SSV with and without MBP. The sample without MBP shows a nearly symmetric signal with a phase transition temperature $T_M = 22.0°C$ and a halfwidth $\Delta T_{1/2}$ that is roughly a factor of four higher than usually obtained for multilamellar vesicles (MLV) of DMPC. This higher halfwidth and the 2 C° lower T_M (as compared to MLV) is characteristic for SSVs and is most likely due to an elevated lateral stress along the plane of the bilayer [9]. The small peak at the right of the endotherm with $T_M = 24.3°C$ arises from vesicles (SUV) in the sample that are not solid supported and were not completely removed by the washing procedure prior to the DSC measurement.

The addition of highly concentrated MBP to this sample has a measurable effect on the endotherm (data not shown). Its high temperature shoulder slightly increases in intensity and the T_M increases by 1.5 C°. This indicates that there is a (presumably weak) interaction of MBP with the phosphatidylcholine headgroup. The weak character of this interaction becomes obvious after washing the sample. This procedure gives rise to the endotherm shown in Fig. 1A by the solid line. It is similar to the original endotherm obtained without MBP with the exception of the small peak at 24.3°C, which has disappeared, indicating that the small fraction of non-supported vesicles and virtually all MBP were removed from the sample by washing.

The introduction of negatively charged phospholipids into the bilayer prior to the addition of MBP gives a significantly different interaction pattern. Fig. 1B shows this for the case of a DMPC SSV containing 10 mol% DMPS while in Figs. 1C and 1D the negatively charged phospholipid is 10 mol% DMPG and 10 mol% DMPA, respectively. In all three cases shown the addition of MBP causes a broadening together with an increase in asymmetry of the endotherm as well as a shift of T_M towards higher temperature. These features are typical for the coupling of a water soluble protein or polypeptide at the surface of an electrically charged bilayer [19,20].

The gradual change of the DSC endotherm with the concentration of MBP is shown in Fig. 2 in the case of DMPS. At low MBP concentrations, an increase in intensity of the high temperature wing can be observed. Further addition of MBP causes a continuous reduction of the intensity of the signal at 22°C until finally (at a MBP concentration of 40%) only a rather symmetric and broad feature with $T_M \approx 25°C$ remains. Washing of this sample in buffer containing 1 M NaCl does not change the endotherm significantly. Similar results were obtained when the samples shown in Figs. 1B and 1D were washed in 1 M NaCl buffer after MBP addition. This provides evidence that each negatively charged phospholipid species studied renders the coupling between MBP and the bilayer surface sufficiently tight so that monovalent cations such as Na^+ cannot detach the protein.

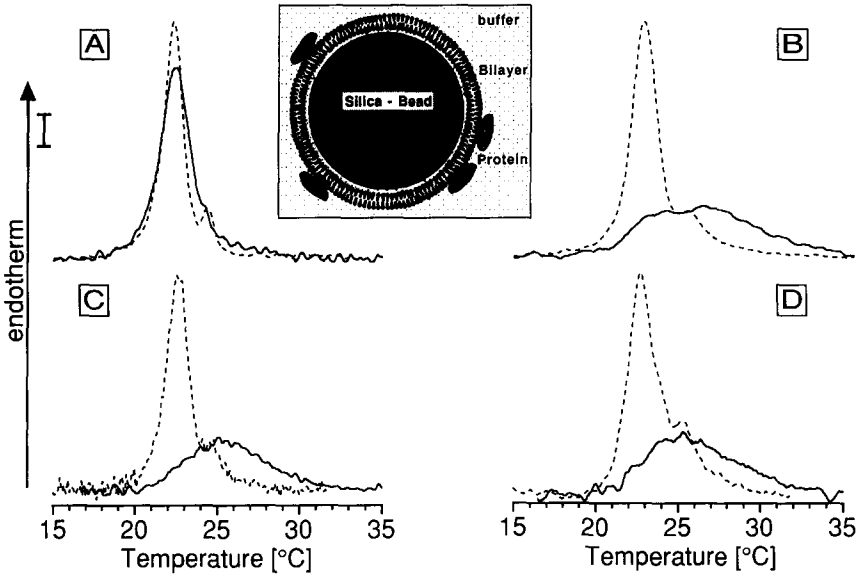

Fig. 1. DSC endotherms of spherical supported vesicles (SSV) of DMPC (A), DMPC/DMPS (10 mol%) (B), DMPC/DMPG (10 mol%) (C) and of DMPC/DMPA (10 mol%) (D) before (dotted lines) and after (full lines) the addition of 50 wt% myelin basic protein. The inset shows a schematic drawing of the model system used for the DSC measurements – the single bilayer on a spherical support (silica bead). The diameter of the spherical support is 640 nm. Scan rate is 30 C°/h.

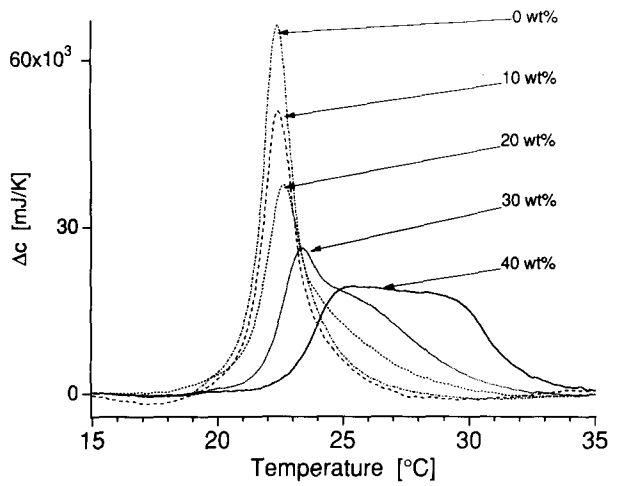

Fig. 2. DSC endotherms of spherical supported vesicles (SSV) of a binary mixture of DMPC with DMPS after the addition of MBP at various concentrations as indicated. Scan rate is 15 C°/h.

FTIR

Fig. 3 shows the variation of the symmetric stretching vibration frequency with temperature of a single bilayer supported by a silicon ATR crystal for two binary mixtures: DMPC-d_{54}/DMPS and DMPC-d_{54}/DMPA. Within the error of the IR frequency determination (error bar in Fig. 3), the transition widths agree with those obtained by DSC, although the IR transition tends to be broader in its wings. Without MBP, the mixing behavior of DMPC-d_{54}/DMPS is nearly ideal, i.e., the melting of both components takes

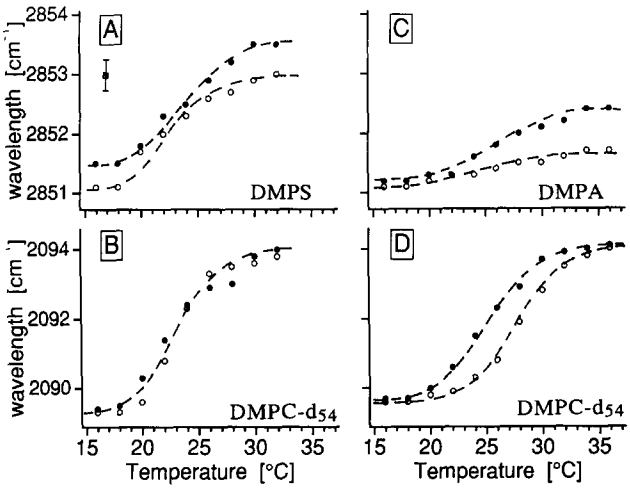

Fig. 3. Temperature dependence of the symmetric stretching vibration frequency of binary mixtures of DMPC-d_{54}/DMPS (A,B) and of DMPC-d_{54}/DMPA (C,D). The samples were prepared as a single bilayer supported by a silicon ATR crystal and were measured before (○) and after (●) flushing the ATR cell assembly with MBP. The components of the DMPC-d_{54}/DMPS (10 mol%) mixture are shown in A (PS) and B (PC) while the components of the DMPC-d_{54}/DMPA (10 mol%) mixture are presented in C (PA) and D (PC). The error bar in A is representative for all measurements. The dotted lines are drawn to guide the eye.

place over a similar temperature range. The PC component of the DMPC-d_{54}/DMPS system exhibits the well known sigmoid shape which does not change significantly after addition of MBP (Fig. 3B). In contrast, the DMPS shows a remarkable broadening of the phase transition at its high temperature shoulder (Fig. 3A) after the addition of MBP. A similar, and even more pronounced effect of MBP on the negatively charged lipid component can be observed with DMPC-d_{54}/DMPA (Figs. 3C and 3D). For this mixture we find that the PC component is slightly affected by the presence of MBP (Fig. 3D). A similar behavior was observed for a DMPC-d_{54}/DMPG mixture, where the presence of MBP causes a broadening of the PG phase transition but does not significantly change the PC transition curve (data not shown).

In general, all three binary mixtures studied exhibit a similar pattern regarding the interaction with MBP. It should be noted that the observed broadening of the phase transition at its high temperature wing is in good agreement with the DSC data. The FTIR now reveals that initially the negatively charged lipid component mainly accounts for this broadening.

For a pure DMPC-d_{54} bilayer no change of the phase transition was observed by FTIR. This is also in agreement with the DSC results, considering the FTIR measurement was performed after thoroughly flushing the ATR cell assembly with buffer in order to remove any 'bulk' MBP that is not bound to the bilayer. This treatment is equivalent to the washing procedure applied to the DSC samples.

The setup of our ATR experiment (as depicted in Fig. 4) offers two unique features. First, the flushing of the cell assembly after addition of the MBP (that removes all MBP dissolved in the bulk solution) allows the determination of the amount of protein bound to the bilayer by simultaneously measuring the amide band intensity of MBP coupled to the bilayer with the signals arising from the lipids. Second, measurements with parallel- and perpendicular-polarized IR permit

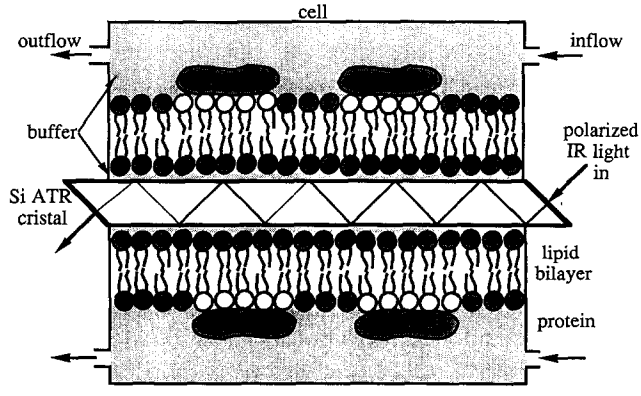

Fig. 4. Schematic drawing of the experimental setup used for the ATR measurements (cf., Materials and Methods for details).

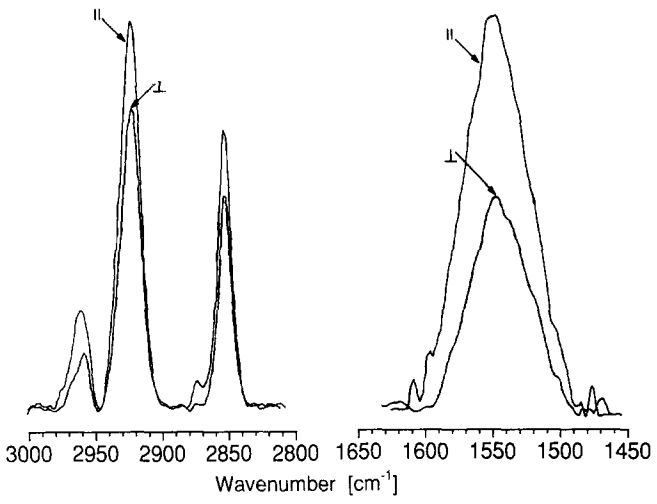

Fig. 5. Polarized FTIR spectra of a single DMPC/DMPA (15 mol%) bilayer on a planar support (silicon ATR crystal) with MBP coupled to the bilayer surface (upper spectrum parallel-polarized, lower spectrum perpendicular-polarized). The CH_2 streching bands (2922 cm^{-1} and 2852 cm^{-1}) of the lipid bilayer and the amide II band (1554 cm^{-1}) of the coupled MBP are shown.

the calculation of the average order parameter $\langle S_{IR} \rangle$ (cf., Eqn. 1) of the lipid chains from the dichroic ratio. Under certain conditions, the average chain tilt angle with respect to the normal direction of the membrane can be calculated according to Eqn. 2.

The sensitivity of our experimental setup for such measurements is illustrated in Fig. 5. The signals shown were obtained after flushing the cell with buffer in order to remove all bulk (non-coupled) MBP. The fact that the signals arise from a single bilayer on the ATR crystal (and from the MBP coupled to it) stresses the very satisfactory sensitivity of our setup. The amide band arising from the MBP was observed only when negatively charged lipids were present in the bilayer but not for a pure DMPC membrane. This again demonstrates the very weak nature of the DMPC–MBP interaction that causes the slight changes of the DSC endotherm (cf., Fig. 1A) and explains why no effect of MBP on the DMPC phase behavior was observed with FTIR. Furthermore, the remarkable dependence of the signal intensities with the polarization of the IR beam suggests that the supported bilayer represents indeed a highly oriented membrane system.

The calculated average order parameters $\langle S_{IR} \rangle$ (Eqn. 1) are listed for both the gel and the liquid-crystalline phase states in Table I. For DMPC-d_{54}, the value of $\beta = 35°$ obtained for the gel phase state agrees within the error of the measurement with results we obtained for a single DMPC bilayer on a solid support employing the neutron specular reflection technique [21]. For low-hydrated multilayers of DMPC in the gel phase, a value of $\beta = 26°$ has been reported recently on the basis of FTIR data [22] while for DPPC multilayers $\beta = 31 \pm 2°$ has been obtained [15]. Our value of $\langle S_{IR} \rangle = 0.50$ for the gel phase of DMPC is significantly lower than $\langle S_{IR} \rangle = 0.78$ obtained for hydrated DPPC multilayers [23]. The value of $\langle S_{IR} \rangle = 0.26$ for the liquid-crystalline phase state of the DMPC bilayer is approx. 40% lower than the one recently obtained for a POPC/POPG (4:1) single supported bilayer by the same technique [17]. It should be noted that for previously reported results on $\langle S_{IR} \rangle$, the bilayer was not facing directly the surface of the support as in our case, which might account for the order parameter discrepancies.

The data in Table I clearly show that the coupling of MBP to a single supported bilayer containing negatively charged lipids is accompanied by a remarkable change of $\langle S_{IR} \rangle$ for both lipid constituents, while for a pure DMPC bilayer no changes can be observed. For the DMPC-d_{54}/DMPS mixture, both lipids exhibit a similar drastic loss of orientational order in the presence of MBP. This can be explained by the nearly ideal mixing behavior of binary systems containing 10–15 mol% DMPG or DMPS (cf., Fig. 1B and Fig. 3). The similar effect on both DMPC-d_{54} and DMPS indicates that the coupling of MBP does not result in the formation of lipid domains containing different amounts of DMPS, neither in the gel phase nor in the fluid phase. Hence, the negative surface charge is presumably smeared over the whole bilayer surface and MBP couples via electrostatic interaction non-specifically.

For DMPC-d_{54}/DMPA the behavior is more complex. Without MBP, both lipids exhibit negative order

TABLE I

Average order parameter $\langle S_{IR} \rangle$ of the lipid constituents of single lipid bilayers on a planar support without and with (values in parentheses) MBP coupled to the bilayer, measured in the gel phase and in the liquid-crystalline phase state, respectively

The error of $\langle S_{IR} \rangle$ and of β is $\Delta\langle S_{IR} \rangle = \pm 0.05$, $\Delta\beta = \pm 3°$ for DMPC-d_{54} and $\Delta\langle S_{IR} \rangle = \pm 0.1$ for the negatively charged lipids DMPS and DMPA.

System	Temp. (°C)	Phase state	$\langle S_{IR} \rangle$	Lipid component
DMPC-d_{54}	16	gel	0.50 (0.50)	
	36	liquid	0.26 (0.26)	
DMPC-d_{54} /DMPS (15 mol%)	16	gel	0.55 (0.35)	PC
	34	liquid	0.43 (0.10)	PC
	16	gel	0.56 (0.30)	PS
	34	liquid	0.26 (0.05)	PS
DMPC-d_{54} /DMPA (15 mol%)	16	gel	−0.16 (0.30)	PC
	36	liquid	−0.18 (0.19)	PC
	16	gel	−0.30 (0.24)	PA
	36	liquid	−0.37 (0.05)	PA

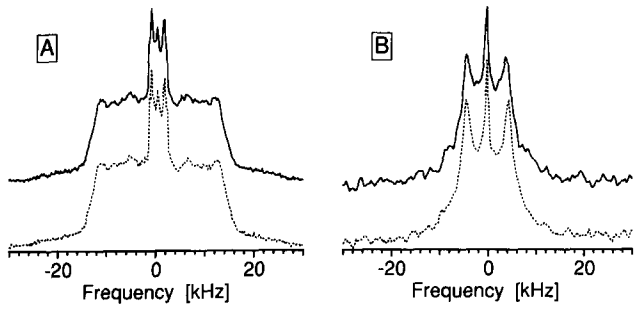

Fig. 6. ^{2}H-NMR spectra of single spherical supported bilayers (dotted lines) and the effect of the addition of 40 wt% MBP (full lines). (A) DMPC-d_{54}, (B) DMPC/DMPG-d_2. The spectra were obtained at a temperature of 35°C.

parameters quite likely a response to the headgroup length mismatch between the two lipids of up to 8 Å together with the ability of DMPA to act as a proton donor for hydrogen bonds. Moreover, the DSC (Fig. 1D) and FTIR data (Fig. 2) indicate that partial demixing occurs in the gel phase. The change of $\langle S_{IR} \rangle$ from negative to positive values due to the MBP coupling indicates that, in the average, the orientation of the lipid long axis (the molecular director axis) tends to orient towards the bilayer normal direction in the presence of MBP.

NMR

^{2}H-NMR experiments performed on single bilayers on a spherical support (SSV, as used for the DSC experiments) enables us to compare the NMR order parameters with those obtained by FTIR. Fig. 6A shows ^{2}H-NMR spectra of single DMPC-d_{54} bilayers on a spherical support (diameter 640 nm) with and without MBP. The well known powder pattern (Pake doublet) arising from the chain deuterons under axially symmetric reorientation and its first moment M_1 do not exhibit any significant changes in the presence of MBP as compared to the control. Hence, the average order parameter $\langle S_{NMR} \rangle$ does not change significantly in the presence of MBP. This finding is in agreement with the FTIR data (Table I). The transverse relaxation time T_2^{qe} was found to be similar for both samples (without and with MBP) at $T_2^{qe} = 190 \pm 10$ μs indicating that the addition of MBP does not result in significant changes of the lateral diffusion of DMPC-d_{54} along the plane of the membrane [14].

A spherical supported bilayer of DMPC-d_{54} with 15 mol% DMPG exhibits a ^{2}H-NMR spectrum indistinguishable from that for pure DMPC-d_{54} (spectrum not shown). The addition of MBP causes minor changes of the NMR lineshape (a slight reduction of the quadrupolar splitting by 5%) but does not change T_2^{qe}. This indicates that the average order parameter $\langle S_{NMR} \rangle$ (cf., Eqn. 3) of the DMPC acyl chains is only slightly reduced due to the coupling of MBP. This result is apparently in contrast to the FTIR data (Table I), where a significant change of $\langle S_{IR} \rangle$ was observed. The reason for this discrepancy is that $\langle S_{NMR} \rangle$ and $\langle S_{IR} \rangle$ describe orientational order on timescales differing by about six orders of magnitude (see discussion below).

An interesting question is whether the MBP coupling to the negatively charged bilayer causes any changes in the headgroup of the negatively charged lipid component, since this part of the molecule is expected to be most directly influenced by the MBP. Fig. 6B shows a ^{2}H-NMR spectrum of SSVs of DMPC with 15 mol% DMPG-d_2 (i.e., the α-methyl group of the DMPG headgroup is deuterated) in the liquid-crystalline phase state. Addition of 40 wt% MBP to this sample causes a slight reduction of the quadrupolar splitting of the α-methylene group by 0.8 kHz (8.8 kHz without MBP) and a significant increase of T_2^{qe} by ≈ 25% while the value of the longitudinal relaxation time T_{1z} remains unchanged at 15 ± 0.5 ms. All NMR data are listed in Table II. While the observed reduction of the quadrupolar splitting of the α-methylene group due to the MBP coupling agrees with the results of an earlier work [3], the increase of T_2^{qe} due to MBP is contrary to the results reported by those authors. They measured a significant decrease of T_2^{qe} for the α-methylene position of phosphatidylglycerol in equimolar DMPC/DMPG-d_5 mixtures due to MBP coupling to MLVs. Indeed, we also observed a decrease of T_2^{qe} of DMPG-d_2 by 30% due to MBP when we used multilamellar vesicles (MLV) instead of SSVs (data not shown). The origin for this behavior is most likely that DMPC MLVs containing DMPG are prone to a macroscopic orientation in the magnetic field [24]. We observed that the MLVs of the DMPC/DMPG-d_2 (20 mol%) mixture exhibit (at 10 Tesla field strength) spectra characteristic for an elliptical distribution of the molecular director axes with a semiaxis ratio of the vesicles of $r_{ex} = 2.5$–2.8 (estimated employing a method

TABLE II

^{2}H-NMR parameters (quadruploar splitting $\Delta\nu_Q$, transverse (T_2^{qe}) and longitudinal (T_{1z}) relaxation times and average order parameter $\langle S_{NMR} \rangle$) for single bilayers on a spherical support (SSV) without and with (values in parentheses) 40 wt% MBP, obtained at a temperature of 35°C

SSV system	$\Delta\nu_Q$ (kHz)	T_2^{qe} (μs)	T_{1z} (ms)	$\langle S_{NMR} \rangle$
DMPC-d_{54}	24 (24)	190 (187)	–	0.15 (0.15)
DMPC-d_{54} / DMPG (15 mol%)	23.4 (22)	194 (200)	–	0.15 (0.14)
DMPC/ DMPG-d_2 (15 mol%)	8.8 (8.0)	185 (241)	15 (15)	–

described in Ref. 13) and with the long axis aligned parallel to the magnetic field. The addition of MBP reduced this eccentricity of the MLVs down to $r_{ex} = 1.5$. As we have demonstrated previously, such a reduction of the partial macroscopic orientation of the MLVs in the magnetic field can account for a more than 30% reduction of T_2^{qe} [13] owing to the anisotropic transverse relaxation caused by lateral diffusion [14,33]. Since the SSVs are not prone to such field orientation at all, the observed increase of T_2^{qe} is likely to reflect changes in the molecular dynamics of the DMPG headgroup correctly while the MLV T_2^{qe} results are dominated by the orientation effect.

The results can be summarized as follows:

(1) MBP strongly interacts electrostatically with DMPC bilayers containing acidic lipids in a similar way for either DMPG, DMPS or DMPA.

(2) Although the protein coupling occurs at one bilayer leaflet only, the whole bilayer responds with changes of its thermodynamic properties and molecular order.

(3) The electrostatic coupling of MBP inhibits the binding of monovalent cations even at very high concentrations of the latter.

(4) ^{2}H-NMR measurements show a significant change of the transverse relaxation time due to MBP coupling.

Discussion

Structural effects of MBP coupling

A salient feature of our DSC (Figs. 1 and 2) and FTIR (Fig. 3) results is that the coupling of MBP causes a shift of the phase transition of the mixture towards higher temperatures, regardless the acidic lipid components used. This is in contradiction to results reported earlier by Boggs et al. [4], where the direction of the temperature shift was found to be dependent on the transition temperatures of the two lipid components. A possible reason for this discrepancy is that they used sonicated vesicles which are well known to exhibit a different phase behavior due to the high curvature of the bilayer [25]. Moreover, changes of the sample morphology owing to the MBP coupling (e.g., vesicles fusion and aggregation) cannot be excluded for sonicated vesicles and might contribute to the shape of the DSC endotherm.

Another interesting feature is that at high MBP concentrations the whole endotherm undergoes an upward shift in temperature (cf., Fig. 2). This indicates that MBP does not cause a demixing in the bilayer by selective interaction with the acidic component, but that both lipids (zwitterionic and acidic) are affected by MBP. A likely mechanism that may be responsible for such a behavior is a partial dehydration of the lipid headgroups due to the interaction with the protein. Dehydration is well known to increase the phase transition temperature and has been observed for the interaction of membrane receptor proteins with negatively charged lipid bilayers [19,20].

Our FTIR order parameter measurements support the conclusion that MBP coupling does not induce demixing. In the gel phase and without MBP, $\langle S_{IR} \rangle$ is similar for both lipids in the DMPC-d_{54}/DMPS mixture but shows significant differences for two components in the DMPC-d_{54}/DMPA system (Table I). Since the mixing behavior in the gel state determines the endotherm shape of a DSC heating scan, these findings should correlate with the DSC results. Indeed, the DSC data show that the system containing DMPA exhibits demixing while a good mixing can be observed for the binary mixture containing DMPS (Fig. 1). MBP coupling renders $\langle S_{IR} \rangle$ similar for all lipids with values of $\langle S_{IR} \rangle = 0.24$–$0.35$, not indicative of demixing. On account of the $\langle S_{IR} \rangle$ values for DMPC-d_{54}/DMPA the MBP coupling seems even to improve the mixing of the two lipids (Table I).

There is another important implication from the finding that the whole endotherm gets shifted upward in temperature due to MBP coupling at high protein concentrations (Fig. 2). Since only one leaflet of the single bilayer is accessible to MBP (the other is oriented to the surface of the solid support), a shift of the whole endotherm indicates that an asymmetric coupling of MBP affects both bilayer leaflets, i.e., there is a strong coupling between the two monolayers via the hydrophobic chain region. A possible redistribution of lipids between the two monolayers as a response to the MBP coupling (e.g., an enrichment of acidic lipids at the interface to the MBP via lipid flip-flop) is not supported by our results. Such a process would cause an increasing tendency towards demixing in the bilayer and $\langle S_{IR} \rangle$ is expected to show significant differences for the two lipid components.

The dominating interaction mechanism of MBP with bilayers

In some previous papers it was suggested on the basis of DSC measurements that MBP partly penetrates into the hydrophobic interior of the bilayer [4,26]. Our DSC results do not support this claim. Hydrophobic interaction of a whole protein or of parts of a protein with the bilayer interior usually leads to a broadening of the endotherm and to a decrease of both liquidus and solidus temperature of the bilayer lipids [20,27]. However, for all binary mixtures studied in this work, an increase of both temperatures was observed upon coupling with MBP by DSC (Fig. 1) and by FTIR (Fig. 3). This is characteristic of an electrostatic interaction with the lipid headgroups [28,29]. The observed changes of the order parameter $\langle S_{IR} \rangle$ due to the MBP coupling are also not indicative for a hydrophobic

interaction since we measured similar changes when polylysine (instead of MBP) interacted with the membrane (data not shown). The interaction of the latter protein is well established to be purely electrostatic in nature [30].

A further indication that the interaction is purely electrostatic in nature is that the NMR results show (in the liquid-crystalline phase state) changes for the DMPG headgroup but not for the hydrophobic chain region in DMPC/DMPG mixtures upon coupling with MBP. In particular, the chain order parameter $\langle S_{NMR} \rangle$ does not change significantly. However, it should be emphasized that the NMR order parameter along the lipid chain is not conclusive for the verification of a protein interaction with the lipid chains. Only changes of the hydrophobic thickness of the membrane (e.g., by interaction with a α-helical peptide causing membrane mismatch) would reflect in the NMR order parameter [31]. A more sensitive proof that no significant interaction between parts of MBP and the lipid chains takes place is the finding that the transverse relaxation time T_2^{qe} obtained for the perdeuterated chains of DMPC does not show any significant change due to MBP coupling to DMPC-d_{54}/DMPG single bilayer.

Although our FTIR results clearly show changes of $\langle S_{IR} \rangle$ due to MBP, we do not attribute this to a hydrophobic interaction. First of all, the values of $\langle S_{IR} \rangle$ are hardly comparable with $\langle S_{NMR} \rangle$ since the very different time scales of the two methods. For NMR, molecular reorientation around the long axis of the lipids is (in the fluid phase) always fast enough, compared to the NMR timescale to average S_{CD} of a single C-D bond along the chain with respect to this axis so that the resulting quadrupolar interaction tensor becomes axially symmetric. Hence, it is the angle β between the long axis and the external magnetic field scaling the quadrupolar frequency. For FTIR, which has a timescale of 10^{-12}–10^{-13} s, this averaging does not in general exist, so that the lipid long axis is not representative of the molecular reorientation anymore. A further complication is that trans-gauche isomerisations in the fluid phase likely occur in a time range similar to the time scale of the method itself. Thus, $\langle S_{IR} \rangle$ is predominantly determined by the instantaneous number of gauche conformers per chain while $\langle S_{NMR} \rangle$ is additionally prone to a static contribution which can reduce its value even further. Hence, $\langle S_{IR} \rangle$ for DMPC-d_{54} is considerably larger than $\langle S_{NMR} \rangle$ (cf., Tables I and II). Therefore we refrained from discussing the changes of $\langle S_{IR} \rangle$ in the fluid phase and did not calculate the tilt angle β.

Dynamical aspects of the MBP–bilayer interaction

The finding that T_2^{qe} of the α-methylene group of DMPG increases due to the interaction with MBP indicates two interesting features. First, since the T_2^{qe} of the DMPC chains in the mixture with DMPG does not change, it clearly shows that the PG headgroup is the primary interaction site for the protein. The observed reduction of the quadrupolar splitting of DMPG is likely caused by a change of the average orientation of the PG headgroup due to the MBP coupling. It should be noted that in a previous paper by Sixl et al. [3] not only was this reduction observed but also a reduction of the splitting of the α-methylene group of the phosphocholine group for a equimolar DMPC/DMPG mixture with MBP. This is in good agreement with our DSC and FTIR results showing that both lipids are influenced by the interaction with MBP (at high MBP concentrations) in a similar fashion. Second, the increase of T_2^{qe} can be an indication for a reduction of the lateral diffusion constant of the acidic lipid by the interaction with the protein. Since T_{1z} does not change, motions being slow on the NMR timescale (such as lateral diffusion of phospholipids) are likely candidates for this T_2^{qe} increase. We demonstrated previously [14,33] that a reduction of the lateral diffusion coefficient D by one order of magnitude causes an increase of T_2^{qe} by a factor of 2. From this we can estimate that the coupling of MBP to the supported bilayer causes a reduction of D by 25–35% for the DMPG, while D for the zwitterionic DMPC remains unaffected. Considering that T_2^{qe} for DMPG represents an average over all PG molecules in the supported bilayer, but that MBP can interact only with 50% of the DMPG (see the above discussion), the reduction of D might be even higher than the above estimate for the DMPG molecules directly affected by the coupling. Recent Monte Carlo simulations by Pink et al. [32] for binary lipid systems of a zwitterionic and an acidic lipid component suggest that – without surmising any lipid domain formation – the reduction of D is indeed a salient feature of the electrostatic interaction of proteins with negatively charged lipid headgroups.

Acknowledgements

We are indebted to Professors Myer Bloom (Vancouver) and David Pink (Halifax) for helpful discussions and to the latter for making his simulation results accessible to us prior to publication. This work was supported by the Sonderforschungsbereich 266 (Project A-1) and by a grant from the Gemeinnützige Hertie Stiftung.

References

1 Boggs, J.M., Moscarello, M.A. and Papahadjopoulos, D. (1982) in Lipid–Protein Interactions (Jost, P.C. and Griffith, O.H., eds.), Vol. 2, pp. 1–51, Wiley-Interscience, New York.
2 Cheifetz, S. and Moscarello, M.A. (1985) Biochemistry 24, 1909–1914.

3 Sixl, F., Brophy, P.J. and Watts, A. (1084) Biochemistry 23, 2032–2039.
4 Boggs, J.M., Wood, D., Moscarello, M.A. and Papahadjopoulos, D. (1977) Biochemistry 16, 2325–2329.
5 Boggs, J.M., Rangaraj, G. and Koshy, K.M. (1988) Biochim. Biophys. Acta 937, 1–8.
6 MacNaughtan, W., Snook, K.A., Caspi, E. and Franks, N.P. (1985) Biochim. Biophys. Acta 818, 132–148.
7 Weise, M.J. (1985) J. Neurochem. 44, 163–170.
8 Tamm, L.K. and McConnel, H.M. (1985) Biophys. J. 47, 105–113.
9 Naumann, C., Brumm, T. and Bayerl, T.M. (1992) Biophys. J. 63, 1314–1319.
10 Bayerl, T.M. and Bloom, M. (1990) Biophys. J. 58, 357–362.
11 Dolainsky, C., Köchy, T., Naumann, C., Brumm, T., Johnson, S.J. and Bayerl, T.M. (1992) in The structure and conformation of amphiphilic membranes (Lipiowsky, R., Richter, D. and Kremer, K., eds.), pp. 34–39, Spinger-Verlag, Berlin.
12 Marassi, F.M. and Macdonald, P.M. (1991) Biochemistry 30, 10558–10566.
13 Brumm, T., Möps, A., Dolainsky, C., Brückner, S. and Bayerl, T.M. (1992) Biophys. J. 61, 1018–1024.
14 Dolainsky, C., Möps, A. and Bayerl, T.M. (1993) J. Chem. Phys. 98, 1712–1721.
15 Fringeli, U.P. (1977) Z. Naturforsch. 32c, 20–45.
16 Harrick, N.J. and Du Pre, F.K. (1966) Appl. Optics 5, 1739–1743.
17 Frey, S. and Tamm, L.K. (1991) Biophys. J. 60, 922–930.
18 Fringeli, U.P. and Gunthard, H.H. (1981) in Membrane Spectroscopy (Grell, E., ed.), pp. 270–332, Springer-Verlag, Berlin.
19 Heise, H., Bayerl, T.M., Isenberg, G. and Sackmann, E. (1991) Biochim. Biophys. Acta 1061, 121–131.
20 Kurrle, A., Rieber, P. and Sackmann, E. (1990) Biochemistry 29, 8274–8281.
21 Johnson, S.J., Bayerl, T.M., McDermott, D.C., Adam, G.W., Rennie, A.R., Thomas, R.K. and Sackmann, E. (1991) Biophys. J., 289–294.
22 Ter-Minassian, L., Okamura, E., Umemura, J. and Takenaka, T. (1988) Biochim. Biophys. Acta 946, 417–423.
23 Okamura, E., Umemura, J. and Takenaka, T. (1990) Biochim. Biophys. Acta 1025, 94–98.
24 Seelig, J., Borle, F. and Cross, T.A. (1985) Biochim. Biophys. Acta 814, 195–198.
25 Lentz, B.R., Carpenter, T.J. and Alford, D.R. (1987) Biochemistry 26, 5389–5397.
26 Boggs, J.M., Moscarello, M.A. and Papahadjopoulos, D. (1977) Biochemistry 16, 5420–5426.
27 Rüppel, D., Kapitzka, H.G., Galla, H.-J., Sixl, F. and Sackmann, E. (1982) Biochim. Biophys. Acta 692, 1–17.
28 Cevc, G., Watts, A. and Marsh, D. (1981) Biochemistry 20, 4955–4965.
29 Dluhy, R.A., Cameron, D.G., Mantsch, H.H. and Mendelson, R. (1983) Biochemistry 22, 6318–6325.
30 Johnson, S.J., Bayerl, T.M., Weihan, W., Noack, H., Penfold, J., Thomas, R.K., Kanellas, D., Rennie, A.R. and Sackmann, E. (1991) Biophys. J. 60, 1017–1025.
31 Nezil, F. and Bloom, M. (1992) Biophys. J. 61, 1176–1183.
32 Pink, D., Ramadurai, K. and Powell, J. (1993) Biochim. Biophys. Acta 1148, 197–208.
33 Köchy, T. and Bayerl, T.M. (1993) Phys. Rev. E 47, in press.